Electrochemical Codeposition of Mg–Li Alloys from a Molten KCl–LiCl–$MgCl_2$ System

Yongde Yan, Milin Zhang,* Wei Han, Yun Xue, Dianxue Cao, and Yi Yuan
Key Laboratory of Superlight Materials and Surface Technology, Ministry of Education, Harbin Engineering University, Harbin 150001, P. R. China

(Received November 20, 2007; CL-071283; E-mail: zhangmilin2007@sina.com)

This work presents a novel study on electrochemical codeposition of Mg–Li alloys on molybdenum in KCl–LiCl (50:50 wt %) melts containing different concentrations $MgCl_2$ at 943 K. Cyclic voltammograms showed that the underpotential deposition (UPD) of lithium on pre-deposited magnesium leads to the formation of liquid Mg–Li alloys. The codepositon of Mg and Li happens when the current intensity exceeds 0.59 A cm^{-2} in KCl–LiCl melts containing 5 wt % $MgCl_2$. α, $\alpha + \beta$, and β phases Mg–Li alloys with different lithium contents were obtained by galvanostatic electrolysis from KCl–LiCl melts with different concentrations $MgCl_2$.

Because of the addition of the lightest metal element lithium into magnesium, it makes magnesium–lithium alloys become the lightest alloys. Mg–Li alloys also show high specific stiffness, high electrical and thermal conductivities. These alloys have been paid great attention owing to their advantages, especially in the aerospace, aircraft, and weapon industry.[1–3]

The traditional method for preparing Mg–Li alloys is mainly mixing pure magnesium and lithium directly. The method has the demerits such as unhomogeneous alloy composition, complicated production process, and high energy waste. Our group has successfully exploited a relatively simpler electrochemical method in which lithium was deposited and diffused to form Mg–Li alloys on magnesium cathode from LiCl–KCl melts at 693–783 K, and electrochemical formation and phase control of Mg–Li alloys were investigated.[4,5] Nevertheless, the shortcomings such as long process and higher energy consumption originating from producing magnesium metal can not be eliminated.

In this work, a new approach is proposed for direct preparation of Mg–Li alloys via electrochemical codeposition of Mg and Li from LiCl–KCl–$MgCl_2$ melts. The process is simpler than those methods mentioned above. The electrochemical codeposition has been widely used to prepare alloys. Ito et al.[6–8] investigated the electrochemical codeposition of Sm–Co alloys from LiCl–KCl–$SmCl_3$–$CoCl_2$ melts, and studied electrochemical formation of Yb–Ni and Sm–Ni alloy films by Li codeposition method from chloride melts. Freyland, Zell and co-workers[9,10] investigated Ni_xAl_{1-x} and Co_xAl_{1-x} alloys via codeposition on Au from the Lewis acid room temperature molten salt. In addition, there are abundant salt lake resources with rich resources of potassium, magnesium, lithium, and boron chlorides in China. The electrodeposition process of magnesium was investigated by some researchers in different molten systems.[11–13] However, the codeposition of Mg–Li alloys has not been reported yet.

The LiCl–KCl mixture (LiCl:KCl = 50:50 (wt %), analytical grade) was contained in an alumina crucible placed in a quartz cell inside a electric furnace. The temperature of melts was measured with a nickel–chromium thermocouple sheathed by an alumina tube. The mixture was carefully pured. All experiments were performed under an argon atmosphere. The electrochemical techniques were performed using *Im*6*e*X electrochemical workstation (Zahner Co., Ltd.). Ag^+/Ag was used as reference electrode, which was constituted by a silver wire ($d = 1$ mm) dipped into a Pyrex tube containing a solution of AgCl (1 wt %) in LiCl–KCl melts. The working electrode was molybdenum wire ($d = 1$ mm). A spectral pure graphite rod ($d = 6$ mm) served as the counter electrode. The active electrode surface was determined after each experiment by measuring the immersion depth of the electrode. The deposits prepared by galvanostatic electrolysis were analyzed by XRD (X' Pert Pro; Philips Co., Ltd.) using Cu Kα radiation at 40 kV and 40 mA. The Mg–Li samples (take 20–50 mg) were dissolved and diluted in aqua regia, then the composition was determined by inductively coupled plasma atomic emission spectrometer (ICP-AES, Thermo Elemental) analysis.

Figure 1 shows typical cyclic voltammograms (CVs) obtained at molybdenum electrodes in LiCl–KCl melts containing different concentrations $MgCl_2$ at 943 K. The cathodic signal B was observed in the LiCl–KCl melts in the absence of $MgCl_2$ in the cathodic limit in curve 1. The cathodic signal B is ascribed to the deposition of Li, since no alloys or intermetallic compounds exist in the Mo–Li binary system at 943 K. In the reverse scan direction, an anodic peak B′ corresponding to the dissolution of Li was observed. After adding 1 wt % $MgCl_2$, peak A associated with reduction of Mg^{II} ions was first detected at about -1.58 V in curve 2. Afterward, a cathodic current was observed. According to the phase diagram of the Mg–Li system,[14] the cathodic current probably corresponds to the formation of a liquid Mg–Li solution which was formed by UPD of lithium on the liquid Mg already deposited on the molybdenum electrode. Because of the high UPD rate of lithium on Mg at relatively high temperatures, a Mg–Li alloy is formed almost from the beginning of the formation of the magnesium phase on the molybdenum substrate. Consequently, the current peak for liquid Mg–Li solution formation is not easy to be detected. Similar phenomenon was observed by Martínez et al.[11] in the eutectic LiCl–KCl melt at 1000 K. In the cathodic limit, peaks B/B′ originated from the deposition/dissolution of Li appeared. In the anodic direc-

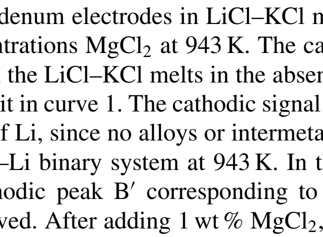

Figure 1. CVs of KCl–LiCl melts at molybdenum electrodes containing different concentrations $MgCl_2$, scan rate: 0.1 V s^{-1}.

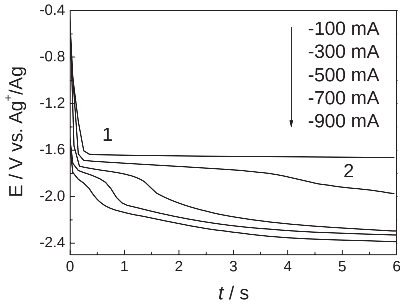

Figure 2. Chronopotentiograms obtained in the LiCl–KCl–$MgCl_2$ (5 wt %) melts with various current intensities at a molybdenum electrode ($S = 0.507\,cm^2$) at 943 K.

tion, peak A′ corresponds to the dissolution of Mg. When the concentration of $MgCl_2$ was increased to 5 wt %, a more pronounced UPD of lithium was observed owing to an increase in the lithium chloride activity ($MgCl_2$ and KCl form complexes K_2MgCl_4).[11]

Figure 2 presents chronopotentiograms of the LiCl–KCl–$MgCl_2$ (5 wt %) melts with different current intensities at a molybdenum electrode ($S = 0.507\,cm^2$). Up to current intensity of 300 mA (current density $0.59\,A\,cm^{-2}$), the curves started to exhibit two potential plateaus (plateaus 1 and 2) associated to the reduction of magnesium and lithium ions into metals, respectively. When the current density exceeds $0.59\,A\,cm^{-2}$, the codeposition of Mg and Li happens. It is obvious that the potential ranges of deposition of Mg and Li are the same as those observed in the CVs.

Based on the results obtained by cyclic voltammetrys and chronopotentiometrys, galvanostatic electrolysis was carried out in LiCl–KCl melts containing different $MgCl_2$ concentrations on molybdenum electrodes at 943 K. For comparison, the molybdenum electrodes with the same active area ($S = 0.322\,cm^2$) were used in electrolysis. Figure 3 shows the XRD patterns of typical α, $\alpha + \beta$, and β phases Mg–Li alloys obtained by galvanostatic electrolysis from the LiCl–KCl melts containing 5, 9, and 10 wt % $MgCl_2$ at 2 A for 2 h, respectively. It is obvious that the lithium contents of Mg–Li alloys decrease (from β to α phase) with the increase of $MgCl_2$ concentrations in the LiCl–KCl melts at constant current intensity. The ICP analyses of all samples obtained by galvanostatic electrolysis are listed in Table 1. Under the same $MgCl_2$ concentration (5 wt %) in the LiCl–KCl melts, the lithium contents of Mg–Li alloys are less when applying lower current intensities. As the $MgCl_2$ concentrations are higher than 10 wt %, the samples prepared by galvanostatic electrolysis at 2 A for 2 h are basically pure Mg. However, when the electrolysis duration was prolonged to 2.5 h, a $\alpha + \beta$ phase Mg–Li alloy (Li 10.75 wt %) was obtained, which indicates the codeposition Mg and Li happens when $MgCl_2$ concentration decreases.

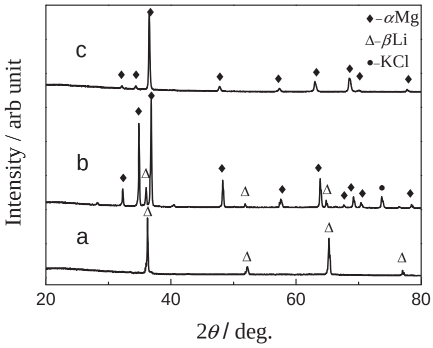

Figure 3. XRD patterns of deposits obtained by galvanostatic electrolysis on Mo electrodes ($S = 0.322\,cm^2$) in the LiCl–KCl melts with $MgCl_2$ of (a) 5 wt %; (b) 9 wt %; (c) 10 wt % at 2 A for 2 h.

Table 1. The ICP analyses of all samples obtained by galvanostatic electrolysis on Mo electrodes ($S = 0.322\,cm^2$) from the LiCl–KCl melts containing different concentrations $MgCl_2$

Samples	$MgCl_2$ concentration /wt %	Current intensity /A	Electrolytic time/h	Li /mg	Mg /mg	Li content /wt %
1	5	0.5	4	8.45	27.5	23.50
2	5	1	2	20.6	14.2	59.19
3	5	2	2	23.4	14.4	61.90
4	8	2	2	3.55	22.4	13.68
5	9	2	2	1.92	22.9	7.74
6	10	2	2	0.056	43.9	0.13
7	10	2	2.5	2.24	18.6	10.75
8	15	2	2	0.013	26.1	0.05
9	20	2	2	0.009	31.8	0.03
10	25	2	2	0.012	29.0	0.04

In conclusion, α, $\alpha + \beta$, and β phases Mg–Li alloys with different lithium contents (0.13–61.90 wt %) were prepared by galvanostatic electrolysis on molybdenum electrode, and the lithium contents of Mg–Li alloys could be controlled by $MgCl_2$ concentration and current density. Mg–Li alloys prepared directly from raw materials of $MgCl_2$ and LiCl will be revolutionary in Mg–Li industry.

The work was financially supported by 863 Project of Ministry of Science and Technology of China (No. 2006AA03Z510), the Scientific Technology Project of Heilongjiang Province (No. GC06A212), and the Scientific Technology Bureau of Harbin (No. 2006PFXXG006).

References

1 G. Y. Sha, Y. B. Xu, E. H. Han, *Mater. Sci. Forum* **2005**, *488*, 717.
2 Z. Drozd, Z. Trojanová, S. Kúdela, *J. Alloys Compd.* **2004**, *378*, 192.
3 A. Sanschagrin, R. Tremblay, R. Angers, D. Dube, *Mater. Sci. Eng., A* **1996**, *220*, 69.
4 M. L. Zhang, Y. D. Yan, Z. Y. Hou, L. A. Fan, Z. Chen, D. X. Tang, *J. Alloys Compd.* **2007**, *440*, 362.
5 M. L. Zhang, Z. Chen, W. Han, Y. Z. Lv, J. Wang, *Chin. Chem. Lett.* **2007**, *18*, 1124.
6 T. Iida, T. Nohira, Y. Ito, *Electrochim. Acta* **2003**, *48*, 2517.
7 T. Iida, T. Nohira, Y. Ito, *Electrochim. Acta* **2003**, *48*, 1531.
8 T. Iida, T. Nohira, Y. Ito, *Electrochim. Acta* **2001**, *46*, 2537.
9 W. Freyland, C. A. Zell, S. Zein El Abedin, F. Endres, *Electrochim. Acta* **2003**, *48*, 3053.
10 C. A. Zell, W. Freyland, *Chem. Phys. Lett.* **2001**, *337*, 293.
11 A. M. Martínez, B. Børesen, G. M. Haarberg, Y. Castrillejo, R. Tunold, *J. Appl. Electrochem.* **2004**, *34*, 1271.
12 Y. Castrillejo, A. M. Martínez, R. Pardo, G. M. Haarberg, *Electrocheim. Acta* **1997**, *42*, 1869.
13 G. M. Rao, *J. Electroanal. Chem.* **1988**, *249*, 191.
14 T. B. Massalski, J. L. Murray, L. H. Benett, H. Baker, *Binary Alloy Phase Diagrams*, American Society for Metals, **1990**.